Carbohydrate Polymers 84 (2011) 292–298

Contents lists available at ScienceDirect

Carbohydrate Polymers

journal homepage: www.elsevier.com/locate/carbpol

Agglomeration mechanisms of cassava starch during pneumatic conveying drying

S. Aichayawanich [a], M. Nopharatana [a,*], A. Nopharatana [b], W. Songkasiri [c]

[a] Food Engineering Department, Faculty of Engineering, King Mongkut's University of Technology Thonburi, 126 Prachautid Road, Bangkok 10140, Thailand
[b] Pilot Plant Development and Training Institute, King Mongkut's University of Technology Thonburi (Bangkhuntien), 83 Moo 8 Thakham, Bangkhuntien, Bangkok 10150, Thailand
[c] National Center for Genetic Engineering and Biotechnology, Excellence Center of Waste Utilization and Management, PDTI Building, 83 Moo 8 Thakham, Bangkhuntien, Bangkok 10150, Thailand

ARTICLE INFO

Article history:
Received 9 July 2010
Received in revised form 2 November 2010
Accepted 17 November 2010
Available online 24 November 2010

Keywords:
Cassava starch
Gelatinization
Glass transition
Particle size
Pneumatic conveying drying

ABSTRACT

This study aimed to investigate the agglomeration mechanisms of cassava starch during pneumatic conveying drying based on phase transition concept. Glass transition and gelatinization temperatures of cassava starch were determined at various starch moisture contents. To investigate phase transition of cassava starch, cassava starch was dried using pilot-scale pneumatic conveying dryer. Temperature, moisture content and particle size distribution of cassava starch were measured along the drying tube. Experimental results showed that at the early stage of drying process, the temperature of cassava starch was higher than its glass transition temperature indicating that the starch was in rubbery phase. After the starch passed the middle stage of drying tube, the phase changed from rubbery to glassy state. This phase transition of the cassava starch correlated with the changes of particle size. The agglomeration of the cassava starch occurred when the cassava starch was in rubbery phase.

1. Introduction

Cassava starch has extensive industrial applications in various industries. Cassava starch production starts with the preparation process in which cassava roots are washed, peeled, and cut into small pieces. Chopped roots are then wet milled to obtain starch slurry. The slurry is sent to the extraction and separation processes to remove pulp and fine fiber, respectively. After that, the slurry is sent to dewatering process. The moist starch is then dried and sent to packing process (Chavalparit & Ongwandee, 2009; Sriroth, Piyachomkwan, Wanlapatit, & Oates, 2000).

Pneumatic conveying drying is a widely used process in cassava starch production. During the drying process, some fractions of the starch agglomerated into large particles. These fractions of the starch have undesired functional properties such as low viscosity, high gelatinization temperature and low acid/enzyme hydrolysis rate (Liu, Wu, Chen, & Chang, 2009; Tang, Ando, Watanabe, Takeda, & Mitsunaga, 2000; Tang, Ando, Watanabe, Takeda, & Mitsunaga, 2001). Moreover, large particles can cause problems in handling process such as during pneumatic transportation process (Boonyai, Bhandari, & Howes, 2004; Özkan, Walisinghe, & Chen, 2002; Turchiuli, Eloualia, Mansouri, & Dumoulin, 2005). These fractions of the starch are then sent to reprocess, resulting in a higher cost of production.

Currently, little is known on the mechanisms of cassava starch agglomeration during pneumatic conveying drying. However, the agglomeration mechanisms of several food powders during drying process were proposed to be two main types – liquid bridge and solid bridge (Adhikari, Howes, Bhandari, & Troung, 2003; Boonyai et al., 2004; Foster, Bronlund, & Pasterson, 2006; Papadakis & Bahu, 1992; Tomas, 2007). Both mechanisms relate to phase transition temperatures of that specific powder. Liquid bridge is generated in amorphous powder when it is at the temperature higher than its glass transition temperature. Its surface changes from a solid-like glassy phase (viscosity of $\approx 10^{12}$ Pa s) to a liquid-like rubbery phase (viscosity of $\approx 10^{6}$–10^{8} Pa s) and becomes sticky. When neighboring powder particles collide, the powder particles agglomeration occurs (Truong, Bhandari, Howes, & Adhikari, 2004). Solid bridge mechanism occurs in solid or crystalline powder at the temperature higher than its melting temperature. The solid or crystalline in the powder particles is melted and forms a bridge at the contact points resulting in the powder particles agglomeration (Nijdam & Langrish, 2006; Papadakis & Bahu, 1992; Tomas, 2007; Viguié, Sukmanowski, Nölting, & Royer, 2007). Cassava starch powder is a semi-crystalline. Its structure composes of amorphous and crystalline region in which glass transition and melting or gelatinization may occur when the particles are in a high temperature condition such as in the drying process (Hoover, 2001; Rickard, Asaoka, & Blanshard, 1991). Liquid bridge and solid bridge may occur between the starch particles during pneumatic conveying drying process.

Currently, there is no scientific method to measure liquid bridge and solid bridge in situ during drying process (Werner, Jones, &

* Corresponding author. Tel.: +66 24709249; fax: +66 24709240.
E-mail address: montira.nop@kmutt.ac.th (M. Nopharatana).

0144-8617/$ – see front matter © 2010 Elsevier Ltd. All rights reserved.
doi:10.1016/j.carbpol.2010.11.036

Table 1
Chemical compositions of the moist cassava starch.

Compositions	Content
Carbohydrate	99.83 g/100 g (dried starch)
Amylose	27.12 g/100 g (dried starch)
Fat	<0.01 g/100 g (dried starch)
Protein	<0.01 g/100 g (dried starch)
Ash	<0.17 g/100 g (dried starch)
Sulfur dioxide	Not detected

Paterson, 2007). Many researchers proposed an alternative method to investigate the mechanism of liquid bridge and solid bridge in powders based on the drying kinetics and phase transition of each powder (Adhikari et al., 2003; Foster et al., 2006; Papadakis & Bahu, 1992; Tomas, 2007). The liquid bridge and solid bridge can be formed, if the drying kinetics of powders is suitable for phase changes. This research, thus, aims to investigate the phase transition temperatures of cassava starch, including glass transition and gelatinization temperatures, using differential scanning calorimetry (DSC). Temperature and moisture content of cassava starch along pneumatic conveying drying were determined at various drying temperatures to determine the drying kinetics. Further, the particle size distribution of cassava starch during pneumatic conveying drying was evaluated in order to propose the possible agglomeration mechanisms.

2. Materials and methods

2.1. Material

Moist cassava starch after the dewatering process was obtained from a cassava starch factory in Chonburi province, Thailand. The chemical compositions of the moist cassava starch were determined following AOAC (1990) methods and percentage of crystallinity of the moist cassava starch were determined using X-ray diffractometer (Rigaku TTRAX III). The moisture content and percentage of crystallinity of the moist cassava starch were approximately $48.00 \pm 3.45\%$ (d.b.) and $38.15 \pm 1.23\%$, respectively. The details of other compositions (g/100 g of dried starch) are shown in Table 1.

2.2. Material preparation

To adjust starch moisture content, moist cassava starch was rewetted in water at the ratio of starch to water of 1:2 (w/w) and left overnight. The starch slurry was placed in 1 μm filter bag and centrifuged using basket centrifuge at $1660 \times g$ for 5 min. The moisture content of moist cassava starch was then adjusted from 8.6 to 25.2% (d.b.) by placing in a desiccating container containing LiCl, KCl, NaCl, KNO_3 and K_2SO_4 saturated solutions at 25 °C. To obtain cassava starch with the moisture content of 30–100% (d.b.), the moist cassava starch was placed over P_2O_5 at 25 °C until the weights were constant. Then, it was rewetted and kept overnight.

2.3. DSC protocol

To determine the glass transition temperature, 13–15 mg of moist cassava starch was placed in a pressure aluminum pan and equilibrated inside the DSC (Mettler Toledo – DSC1) at −50 °C for 5 min, using an empty pan as a reference. Then, the sample was heated at 10 °C/min from −50 to 170 °C. Depending on the sample moisture contents, different final temperature was used, to protect the sample from gelatinization process. Each sample was scanned twice. The second scanning was performed to reduce the enthalpy relaxation of the sample which appears in the first scan. The glass transition temperature was determined at the second scan.

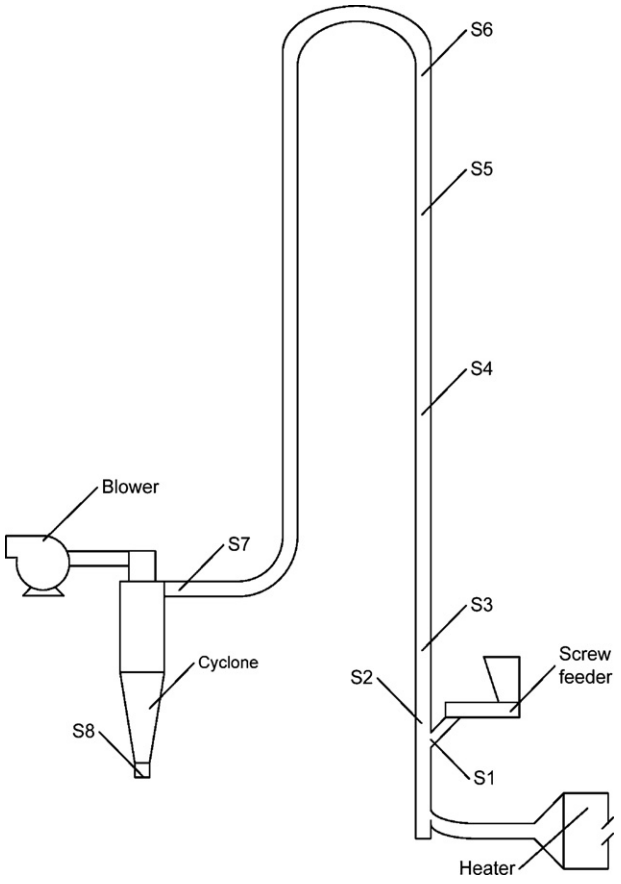

Fig. 1. Schematic diagram of pilot-scale pneumatic conveying dryer; S1–S8 are sampling points.

To determine the gelatinization temperature, 13–15 mg of moist cassava starch was sealed in a pressure aluminum pan and scanned against a reference empty pan using the DSC from 25 to 170 °C at 10 °C/min scanning rate.

2.4. Determination of temperature and moisture profiles along the pneumatic conveying dryer

Fig. 1 presents schematic diagram of a pilot-scale pneumatic conveying dryer used in this research. After passing an electrical heater, hot drying air was flowed along the cylindrical drying tube with 9.70 m of length and 0.07 m of inner diameter. In order to facilitate the air flow, a blower was placed at the end of drying tube. During drying, a screw feed was used to continuously convey moist starch into the drying tube. After drying, the dried starch was then separated from the drying air by using cyclone positioning in front of the blower.

Cassava starch with 60% (d.b.) moisture content was fed into the pneumatic conveying dryer at the inlet drying air temperatures of 120, 160, and 200 °C. The inlet drying air velocity was controlled at 20 m/s. After the outlet drying air temperature remained constant, dried cassava starch samples were then collected at 0, 0.05, 0.40, 1.80, 2.70, 3.80, 9.20, and 9.70 m along the dryer tube (S1–S8 in Fig. 1) using a thief probe, which consists of two concentric pipes. By rotating the inner pipe over 90°, the dried cassava starch was trapped. The temperature of dried cassava starch samples were determined immediately using a laser radiation thermocouple (Fluke-62 Mini IR thermometer). The moisture content of the dried starch samples were determined following AOAC (1990)

Table 2
Glass transition temperature of cassava starch at various moisture contents.

Moisture content % (d.b.)	Glass transition temperature (°C)*		
	Onset	Mid point	End point
100.0	Not detected	Not detected	Not detected
60.0	Not detected	Not detected	Not detected
40.0	Not detected	Not detected	Not detected
30.0	$33.94^{f} \pm 0.02$	$34.26^{f} \pm 0.01$	$35.79^{e} \pm 0.03$
25.2	$43.35^{e} \pm 0.05$	$44.69^{e} \pm 0.10$	$45.13^{d} \pm 0.13$
23.1	$46.07^{d} \pm 0.06$	$47.21^{d} \pm 0.15$	$48.47^{c} \pm 0.12$
21.3	$54.71^{c} \pm 0.03$	$56.35^{c} \pm 0.02$	$59.45^{b} \pm 0.04$
13.0	$94.52^{b} \pm 0.02$	$97.58^{b} \pm 0.02$	$105.32^{a} \pm 0.03$
8.6	$132.20^{a} \pm 0.05$	$144.70^{a} \pm 0.09$	$159.43^{a} \pm 0.11$

* Values followed by the same letter are not significantly different ($P \geq 0.05$).

method and calculated from Eq. (1).

$$\text{Moisture content (\% d.b.)} = \frac{W - D}{D} \quad (1)$$

where, W is the wet weight of the material and D is the dry weight of material.

2.5. Determination of particle size distribution along the pneumatic conveying dryer

Particle size distribution was evaluated by the method modified from Jinapong, Suphantharika, and Jamnong (2008). The moisture content of dried cassava starch samples collected from various sampling points were adjusted to 0.53 ± 0.01% (d.b.) by placing them over P_2O_5 at 25 °C until their weights were constant. Then, the particle size distribution was determined using a laser diffraction particle size analyzer (Mastersizer S, Malvern Instruments Ltd.) with a Scirocco 2000 dry powder feeder unit.

2.6. Statistical analysis

The experiment was performed with three replications. The variance was determined by ANOVA and the difference of mean values was determined by Duncan's test. Values were considered at 95% significant ($P < 0.05$).

3. Results and discussions

3.1. Glass transition temperature of cassava starch

Table 2 shows glass transition temperature of cassava starch samples at the moisture contents of 8.6–100% (d.b.). The result showed that glass transition of cassava starch could not be detected in the samples with moisture content higher than 40% (d.b.) due to the effect of ice melting during DSC experiment. However, from the data in Table 2 and DSC curves of glass transition in Fig. 2, at the starch moisture content lower than 40% (d.b.), the result indicated that the glass transition temperatures, including onset, mid point, and end point, significantly decreased when the moisture content of cassava starch increased due to the plasticizing effect of water, which gives more free volume to starch chains (Katekawa & Silva, 2007; Roos, 1995; Slade & Levine, 1988). A similar trend was reported by Perdomo et al. (2009) who studied the effect of moisture content on glass transition temperature of commercial cassava starch at a lower moisture content ranged from 2 to 22% (d.b.). They reported that, when moisture content of the samples was higher than 11% (d.b.), the plasticizing effect of water was evident and glass transition temperature of the samples increased. However, at the same moisture content, glass transition temperatures of cassava starch reported by Perdomo et al. (2009) were slightly different from those in this research. This may be attributed to the different botanical origin of cassava.

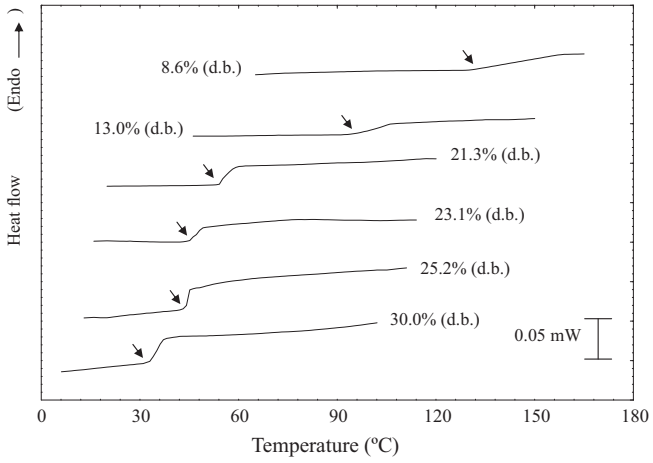

Fig. 2. Typical DSC curves, as a function of glass transition temperature for cassava starch with different moisture contents.

The glass transition temperature of foods and biological materials as a function of weight fraction of water is commonly modeled using Gordon–Taylor equation as shown in Eq. (2) (Gordon & Taylor, 1952).

$$T_g = \frac{w_1 T_{g1} + k T_{g2} w_2}{w_1 + k w_2} \quad (2)$$

where, T_g is glass transition temperature of food material (°C); w_1 is weight fraction of food material; w_2 is weight fraction of water; T_{g1} is glass transition temperature of dry material (0% of moisture content) (°C); T_{g2} is glass transition temperature of water (−135 °C), and k is constant value. From the data in Table 2, the percentages of moisture content of cassava starch were converted to weight fraction and the onset points of glass transition were used to calculate glass transition temperature of dried cassava starch (T_{g1}) and constant value (k). The goodness of fit was evaluated by the determination coefficient (R^2). The result showed that glass transition temperature of dried cassava starch (T_{g1}) was 216.41 °C and k was 3.88 with R^2 of 0.993. The w_1 value in Eq. (2) was replaced by $(1 - w_2)$ and the equation was rearranged as shown in Eq. (3).

$$T_g = \frac{(1 - w_2) T_{g1} + k T_{g2} w_2}{1 + (k - 1) w_2} \quad (3)$$

The predicted equation of the glass transition temperatures of cassava starch is shown in Eq. (4)

$$T_g = \frac{216.41 - 740.21 w_2}{1 + 2.88 w_2} \quad (4)$$

Whittam, Noel, and Ring (1990) determined T_{g1} of A-type crystalline anhydrous starch at 297 °C. Roos and Karel (1991) reported that the T_{g1} of wheat starch was estimated to be 243 °C based on the Fox and Flory equation. The lower T_{g1} of cassava starch in this research is due to the differences in chemical composition of starches (Sablani, Bruno, Kasapis, & Symaladevi, 2009).

3.2. Gelatinization temperature of cassava starch

During starch gelatinization, starch granules adsorb water and swell resulted in a disorder of crystalline region (Hoover, 2001; Rickard et al., 1991). As shown in Table 3, gelatinization of cassava starch was only detected in the samples with moisture content higher than 30% (d.b.). A similar trend was reported by Udomrati, Poolkasorn, Potisate, and Charoenrein (2003) who stated that rice starch required a certain amount of minimum water for gelatinization. The minimum water is approximately 28.95–31.35%, whereas the water content sufficient to complete gelatinization of rice starch

Table 3
Gelatinization temperature of cassava starch at various moisture contents.

Moisture content % (d.b.)	Gelatinization temperature (°C)*		
	Onset	Mid point	End point
100.0	$66.59^{d} \pm 0.01$	$74.49^{d} \pm 0.02$	$82.32^{d} \pm 0.02$
60.0	$70.03^{c} \pm 0.02$	$81.13^{c} \pm 0.01$	$96.26^{c} \pm 0.01$
40.0	$92.86^{b} \pm 0.01$	$108.30^{b} \pm 0.01$	$120.36^{b} \pm 0.02$
30.0	$102.89^{a} \pm 0.03$	$117.44^{a} \pm 0.04$	$132.21^{a} \pm 0.01$
25.2	Not detected	Not detected	Not detected
23.1	Not detected	Not detected	Not detected
21.3	Not detected	Not detected	Not detected
13.0	Not detected	Not detected	Not detected
8.6	Not detected	Not detected	Not detected

* Values followed by the same letter are not significantly different ($P \geq 0.05$).

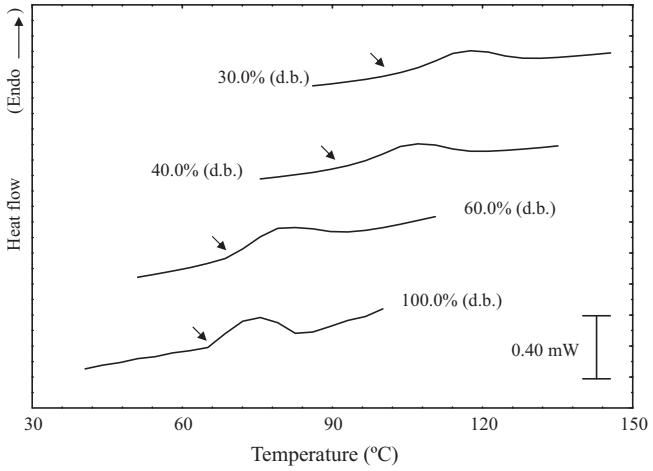

Fig. 3. Typical DSC curves, as a function of gelatinization temperature for cassava starch with different moisture contents.

is around 58–60%. At low moisture content, water in the starch granule is sufficient for softening the amorphous region. At high moisture content, some fraction of water separates from the starch granule. This fraction of water acts as pure solvent and causes gelatinization of starch crystallite. Only starch containing sufficient amount of water can gelatinize (Biliaderis, Page, Maurice, & Juliano, 1986).

From the data in Table 3 and DSC curves of gelatinization in Fig. 3, the gelatinization temperature of cassava starch slightly decreased with increasing moisture content. Evans and Haisman (1982) proposed that increased amount of water facilitates the gelatinization by lowering the melting point of crystallite region. Therefore, as water becomes limiting, gelatinization temperature increased.

Gelatinization temperature of starch as a function of volume fraction of water is often determined using Flory–Huggins equation as shown in Eq. (5) (Farhat & Blanshard, 1997).

$$\frac{1}{T_m} = \frac{RV_u}{\Delta H_u V_1}(\nu_1 - \chi_1 \nu_1^2) + \frac{1}{T_m^o} \quad (5)$$

where T_m is the melting point of starch (K); R is the gas constant; T_m^o is the melting point of dry starch; υ_1 is the volume fraction of water; V_u/V_1 is the ratio of the molar volumes of repeating unit in the chain to that of water; ΔH_u is the change in the enthalpy of fusion per repeating unit, and χ_1 is the interaction parameter (K^{-1}). Eq. (5) can be modified as Eq. (6), where, α is $RV_u/\Delta H_u V_1$.

$$\frac{1}{T_m} = \alpha(\nu_1 - \chi_1 \nu_1^2) + \frac{1}{T_m^o} \quad (6)$$

From the data in Table 3, the onset of gelatinization temperatures were used to calculate gelatinization temperature of dried cassava starch (T_m^o), α and χ_1 value. The gelatinization temperature of dried cassava starch (T_m^o) was 529.40 K (or 256.40 °C). α and χ_1 values equal to $4.27 \times 10^{-3}\ K^{-1}$ and 0.99, respectively. The predicted equation of the gelatinization temperatures of cassava starch is shown in Eq. (7) with an R^2 value of 0.986. The T_m^o value of dried cassava starch in this research is closed to the result of Whittam et al. (1990) who studied melting behavior of A- and B-type crystalline starch and reported that the gelatinization temperature of the dried crystalline starch was 530 K as calculated from Flory–Huggins equation.

$$\frac{1}{T_m} = 0.00427(u_1 - 0.99u_1^2) + 0.00189 \quad (7)$$

3.3. Phase of cassava starch during pneumatic conveying drying

Table 4 shows the temperature and moisture profiles of cassava starch samples along the pneumatic conveying drying tube at the drying air temperatures of 120, 160, and 200 °C. During drying, the temperature of cassava starch samples continuously increased along the drying tube, while the moisture content of the samples reduced. The final temperatures of the samples dried with drying air temperature of 120, 160, and 200 °C were 38.47, 44.99, and 52.97 °C and their final moisture contents were 12.18, 11.91, and 10.99% (d.b.), respectively. The final moisture contents decreased when the drying air temperature increased.

To investigate the phase transition of cassava starch during pneumatic conveying drying, the temperature profiles of cassava starch samples along the drying tube were compared with the predicted glass transition and gelatinization temperatures obtained from Eqs. (4) and (7) as shown in Fig. 4. The results revealed that the temperature of all cassava starch samples remains lower than its gelatinization temperature throughout the drying period. This indicated that gelatinization did not occur during drying. However, at sampling point 1 or the feeder, the temperature of starch samples was lower than its glass transition temperature indicat-

Table 4
Temperature and moisture content of cassava starch along the pneumatic conveying drying tube at the drying air temperatures of 120, 160, and 200 °C.

Sampling points	Cassava starch samples					
	Drying air temperature of 120 °C		Drying air temperature of 160 °C		Drying air temperature of 200 °C	
	Temperature (°C)	Moisture content % (d.b.)	Temperature (°C)	Moisture content % (d.b.)	Temperature (°C)	Moisture content % (d.b.)
S1	28.33 ± 0.23	60.02 ± 1.91	28.33 ± 0.23	60.02 ± 1.91	28.33 ± 0.23	60.02 ± 1.91
S2	35.30 ± 0.34	58.86 ± 1.33	38.52 ± 0.45	58.10 ± 0.34	41.90 ± 0.36	58.67 ± 1.24
S3	35.41 ± 1.22	37.82 ± 0.32	38.98 ± 0.78	36.69 ± 0.32	43.93 ± 0.81	34.90 ± 0.90
S4	35.52 ± 0.43	34.30 ± 0.99	39.83 ± 0.55	33.00 ± 0.52	47.37 ± 0.42	30.42 ± 0.17
S5	36.64 ± 0.96	30.93 ± 0.32	40.52 ± 0.43	29.53 ± 0.23	48.03 ± 0.80	27.86 ± 0.85
S6	37.33 ± 0.57	22.51 ± 0.57	42.43 ± 0.98	21.94 ± 1.00	49.20 ± 0.40	21.03 ± 0.20
S7	37.60 ± 0.78	17.20 ± 0.65	43.50 ± 1.02	16.82 ± 0.13	51.07 ± 0.30	15.95 ± 0.24
S8	38.47 ± 0.78	12.18 ± 0.77	44.99 ± 0.56	11.91 ± 0.87	52.97 ± 0.87	10.99 ± 0.91

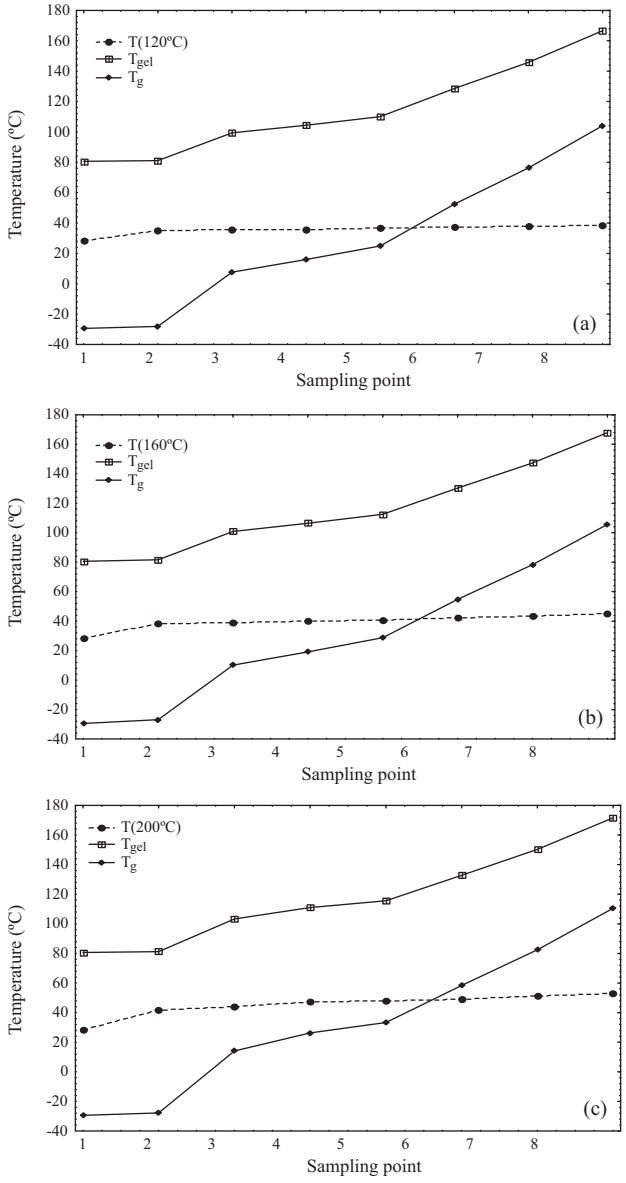

Fig. 4. Glass transition temperature, gelatinization temperature and temperature profile of cassava starch along the pneumatic conveying drying tube at various drying air temperatures of (a) 120 °C; (b) 160 °C; and (c) 200 °C.

ing that the samples were in rubbery phase before drying. During drying, the starch samples remained in rubbery phase until the samples flowed pass sampling point 5. Between sampling points 5 and 6, the temperature of the starch samples was higher than its glass transition temperature which indicated that the starch samples changed from rubbery to glassy phase. After that the starch samples remained in glassy phase unit the end of drying process.

3.4. Particle size of cassava starch during pneumatic conveying drying

Particle size distribution of cassava starch along the drying tube at the drying air temperatures of 120, 160, and 200 °C were determined (shown in Table 5). D10, D50, and D90 value are defined as 10, 50, and 90% volume less than or equal to D, respectively. The D10, D50, and D90 values strongly increased in the beginning of drying period which indicated that cassava starch is agglomerate in to large particles. However, the D10, D50, and D90 values decreased after the samples flowed pass the sampling point 2. This finding revealed that agglomerated cassava starch particles can break into small particles. Kalman (1999) studied the attrition of materials during pneumatic conveying and suggested that, during materials flowing in the tube, the particle size of agglomerated materials decreased when the agglomerated particle of material experienced impact/shear load from collision between the agglomerated particles and collide against the tube wall with the higher impact/shear load than the agglomerated strength of the particles.

3.5. Relation between particle size and phase of cassava starch during pneumatic conveying drying

The difference between cassava starch temperature and its glass transition temperature ($T_{\text{cassava starch}} - T_g$) was used to describe phase of cassava starch. The positive value indicated that cassava starch is in rubbery phase, while the negative value revealed that cassava starch is in glassy phase. The higher positive value indicated that phase of cassava starch has high rubber characteristic while the higher negative value indicated that phase of cassava starch has high glass characteristic.

($T_{\text{cassava starch}} - T_g$) values of cassava starch along the pneumatic conveying dryer tube were compared with the particle sizes (D90 value) as shown in Fig. 5. The plot showed that the profiles of ($T_{\text{cassava starch}} - T_g$) values correlated with the profiles of D90 values. From the profiles, the drying tube can be divided into three zones. In zone I, ($T_{\text{cassava starch}} - T_g$) values was positive and increased while the D90 values also increased. Cassava starch particles were in rubbery phase and had higher rubber characteristic than that before drying so they are strongly agglomerated into large particle. The agglomeration mechanism may be liquid bridge formation. In zone II which is in the middle of drying tube ($T_{\text{cassava starch}} - T_g$) and D90 values decreased. Cassava starch particles remained in rubbery phase. However, the particles had a lower rubber characteristic as the ($T_{\text{cassava starch}} - T_g$)

Table 5
Particle size distribution of dried cassava starch along the pneumatic conveying dryer tube.

Sampling points	Cassava starch samples								
	Drying air temperature of 120 °C			Drying air temperature of 160 °C			Drying air temperature of 200 °C		
	D10	D50	D90	D10	D50	D90	D10	D50	D90
S1	8.37 ± 1.02	21.47 ± 0.08	108.46 ± 2.63	8.37 ± 1.02	21.47 ± 0.08	108.46 ± 2.63	8.37 ± 1.02	21.47 ± 0.08	108.46 ± 2.63
S2	9.83 ± 0.89	30.44 ± 0.32	385.99 ± 0.34	10.36 ± 0.23	35.37 ± 2.98	498.01 ± 0.49	10.77 ± 1.32	40.21 ± 0.68	539.13 ± 3.81
S3	9.14 ± 0.55	25.27 ± 0.54	364.25 ± 1.05	10.00 ± 1.04	32.15 ± 2.09	458.43 ± 0.19	10.08 ± 0.21	36.58 ± 2.40	475.78 ± 2.67
S4	9.00 ± 0.43	25.00 ± 0.56	342.52 ± 0.54	9.93 ± 1.90	29.28 ± 1.15	413.68 ± 0.04	9.97 ± 0.32	35.53 ± 1.89	467.54 ± 4.93
S5	8.98 ± 0.53	24.79 ± 0.12	325.47 ± 0.99	9.71 ± 0.43	28.99 ± 0.34	390.01 ± 1.05	9.89 ± 1.02	34.61 ± 0.66	436.50 ± 2.31
S6	8.76 ± 0.56	24.32 ± 0.17	238.43 ± 1.98	9.70 ± 0.45	27.63 ± 0.45	289.16 ± 0.44	9.96 ± 0.98	34.03 ± 0.43	417.03 ± 2.56
S7	8.66 ± 0.10	23.25 ± 0.19	163.38 ± 3.69	9.04 ± 0.52	28.01 ± 1.43	258.43 ± 8.45	9.54 ± 0.34	29.48 ± 1.12	321.07 ± 5.34
S8	8.42 ± 0.11	21.28 ± 0.42	103.33 ± 4.26	8.98 ± 0.98	25.25 ± 0.37	234.21 ± 6.36	8.75 ± 0.56	28.86 ± 1.11	265.10 ± 0.34

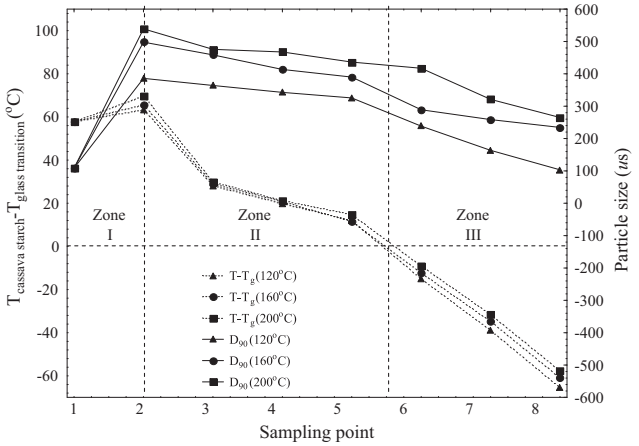

Fig. 5. ($T_{\text{cassava starch}} - T_g$) and particle sizes (D90) values of cassava starch drying at drying air temperatures of 120, 160, and 200 °C along the pneumatic conveying drying tube.

decreased. This resulted in the breakage of agglomerated particles into small particles or a granule. Verdurmen, Houwelingen, Gunsing, Verschueren, and Stratsma (2006) explained that if the impact/shear loads from the collision force between the particles are higher than the attractive force from liquid bridge between the starch granules in the particle, agglomerated particles can be broken. Zone III occurred at the end of drying tube where the ($T_{\text{cassava starch}} - T_g$) values were negative and decreased while the D90 values also decreased. Cassava starch was in glassy phase and had brittle characteristics. Therefore, the agglomerate particles were easily broken. Moreover, the bend tube was established at this zone (between sampling points 6 and 8 as in Fig. 1). When cassava starch flowed pass this zone, the collision force between the starch particles and tube wall may cause the breakage of starch particles.

The results in Fig. 5 also showed that, the positive value of ($T_{\text{cassava starch}} - T_g$) of cassava starch dried at 200 °C was the highest. However, the negative value of ($T_{\text{cassava starch}} - T_g$) of starch dried at 200 °C was the lowest. This implied that at the drying air temperature of 200 °C, the starch had higher rubber characteristic when they were in zone I and II and lower glass characteristic when they were in zone III. Therefore, the D90 values of the starch dried at 200 °C was higher than that of cassava starch dried at lower drying air temperatures (Fig. 5).

4. Conclusion

Phase and agglomeration of cassava starch during pneumatic conveying drying were investigated. The agglomeration mechanisms of the starch were then proposed. It was found that the phase transition correlated with starch agglomeration during drying. When the starch phase was in rubbery phase, the agglomeration of the starch particles increased. However, the agglomeration of the starch decreased when the starch phase was in glassy phase. This indicated that the agglomeration mechanism of the starch is the result of liquid bridge formation. In order to reduce the starch agglomeration by liquid bridge formation during the drying process, the starch should be dried at temperature lower than its glass transition temperature.

Acknowledgements

The authors would like to thank the Commission on Higher Education, Thailand for supporting by grant fund under the program Strategic Scholarships for research. Frontier Research Network for the Ph.D. Program Thai Doctoral degree for this.

References

Adhikari, B., Howes, T., Bhandari, B. R., & Troung, V. (2003). Surface stickiness of drops of carbohydrate and organic acid solutions during convective drying: Experiments and modeling. *Drying Technology*, *21*(5), 839–873.
AOAC. (1990). *Official methods of analysis* (14th ed.). Washington, DC: Association of Official Analytical Chemists.
Biliaderis, C. G., Page, C. M., Maurice, T. J., & Juliano, B. (1986). Thermal characterization of rice starches: A polymeric approach to phase transitions of granular starch. *Journal of Agricultural and Food Chemistry*, *34*(1), 14–17.
Boonyai, P., Bhandari, B., & Howes, T. (2004). Stickiness measurement techniques for food powders: A review. *Powder Technology*, *145*, 34–46.
Chavalparit, O., & Ongwandee, M. (2009). Clean technology for the tapioca starch industry in Thailand. *Journal of Cleaner Production*, *17*, 105–110.
Evans, I. D., & Haisman, D. R. (1982). The effect of solutes on the gelatinization temperature range of potato starch. *Starch*, *34*, 224–231.
Farhat, I. A., & Blanshard, J. M. V. (1997). On the extrapolation of the melting temperature of dry starch from starch–water data using the Flory–Huggins equation. *Carbohydrate Polymers*, *97*, 263–265.
Foster, K. D., Bronlund, J. E., & Pasterson, A. H. J. (2006). Glass transition related cohesion of amorphous sugar powders. *Journal of Food Engineering*, *77*, 997–1006.
Gordon, M., & Taylor, J. (1952). Ideal copolymers and the second-order transitions of synthetic rubbers. I. Non-crystalline copolymers. *Journal of Applied Chemistry*, *2*, 493–500.
Hoover, R. (2001). Composition, molecular structure, and physicochemical properties of tuber and root starches: A review. *Carbohydrate Polymers*, *45*, 253–267.
Jinapong, N., Suphantharika, M., & Jamnong, P. (2008). Production of instant soymilk powders by ultrafiltration, spray drying and fluidized bed agglomeration. *Journal of Food Engineering*, *84*, 194–205.
Kalman, H. (1999). Attrition control by pneumatic conveying. *Powder Technology*, *104*, 214–220.
Katekawa, M. E., & Silva, M. A. (2007). On the influence of glass transition on shrinkage in convective drying of fruits: A case study of banana drying. *Drying Technology*, *25*, 1659–1666.
Liu, D., Wu, Q., Chen, H., & Chang, P. R. (2009). Transitional properties of starch colloid with particle size reduction from micro- to nanometer. *Journal of Colloid and Interface Science*, *339*(1), 117–124.
Nijdam, J. J., & Langrish, T. A. G. (2006). The effect of surface composition on the functional properties of milk powders. *Journal of Food Engineering*, *77*, 919–925.
Özkan, N., Walisinghe, N., & Chen, X. D. (2002). Characterization of stickiness and cake formation in whole and skim milk powders. *Journal of Food Engineering*, *55*, 293–303.
Papadakis, S. E., & Bahu, R. E. (1992). The sticky issues of drying. *Drying Technology*, *10*(4), 817–837.
Perdomo, J., Cova, A., Sandoval, A. J., García, L., Laredo, E., & Müller, A. J. (2009). Glass transition temperatures and water sorption isotherms of cassava starch. *Carbohydrate Polymers*, *76*, 305–313.
Rickard, J., Asaoka, M., & Blanshard, J. (1991). The physicochemical properties of cassava starch. *Tropical Science*, *31*, 189–207.
Roos, Y. H. (1995). *Phase transition in foods*. San Diego: Academic Press., pp. 73–107.
Roos, Y. H., & Karel, M. (1991). Water and molecular weight effects on glass transition in amorphous carbohydrates and carbohydrate solutions. *Journal of Food Science*, *56*, 1676–1681.
Sablani, S. S., Bruno, L., Kasapis, S., & Symaladevi, R. M. (2009). Thermal transitions of rice: Development of a state diagram. *Journal of Food Engineering*, *90*, 110–118.
Slade, L., & Levine, H. (1988). Structural stability of intermediate moisture foods. A new understanding. In J. M. V. Blanshard, & J. R. Mitchell (Eds.), *Food structure: Its creation and evaluation* (pp. 115–147). London: Butterworths.
Sriroth, K., Piyachomkwan, K., Wanlapatit, S., & Oates, C. (2000). Cassava starch technology: The Thai experience. *Stärke*, *52*, 439–449.
Tang, H., Ando, H., Watanabe, K., Takeda, Y., & Mitsunaga, T. (2000). Some physicochemical properties of small-, medium-, and large-granule starches in fractions of waxy barley grain. *Cereal Chemistry*, *77*(1), 27–31.
Tang, H., Ando, H., Watanabe, K., Takeda, Y., & Mitsunaga, T. (2001). Physicochemical properties and structure of large, medium and small granules starches in fractions of normal barley endosperm. *Carbohydrate Research*, *330*, 241–248.
Tomas, J. (2007). Adhesion of ultrafine particles – A micromechanical approach. *Chemical Engineering Science*, *62*, 1997–2010.
Truong, V., Bhandari, B. R., Howes, T., & Adhikari, B. (2004). Glass transition behavior of fructose. *International Journal of Food Science and Technology*, *39*, 569–578.
Turchiuli, C., Eloualia, Z., Mansouri, N. E., & Dumoulin, E. (2005). Fluidised bed agglomeration: Agglomerates shape and end-use properties. *Powder Technology*, *157*, 168–175.
Udomrati, S., Poolkasorn, K., Potisate, S., & Charoenrein, S. (2003). Effects of water content on gelatinization of various rice flours. In *Proceedings of 41st Kasetsart University Annual Conference* Bangkok, Thailand, February 3–7, (Subject: Agro-Industry).
Verdurmen, R. E. M., Houwelingen, G., Gunsing, M., Verschueren, M., & Stratsma, J. (2006). Agglomeration in spray drying installations (The EDECAD Project):

Stickiness measurement and simulation results. *Drying Technology*, *24*, 721–726.
Viguié, J., Sukmanowski, J., Nölting, B., & Royer, F. (2007). Study of agglomeration of alumina nanoparticles by atomic force microscopy (AFM) and photon correlation spectroscopy (PCS). *Colloids and Surfaces*, *302*, 269–275.
Werner, S. R. L., Jones, J. R., & Paterson, A. H. J. (2007). Stickiness during drying of amorphous skin-forming solutions using a probe tack test. *Journal of Food Engineering*, *81*, 647–656.
Whittam, M. A., Noel, T. R., & Ring, S. G. (1990). Melting behaviour of A- and B-type crystalline starch. *International Journal of Biological Macromolecules*, *12*, 359–362.